



Published in final edited form as:

Endocrinology. 2007 January ; 148(1): 116. doi:10.1210/en.2006-0561.

Exposure to Environmentally Relevant Doses of the Xenoestrogen Bisphenol-A Alters Development of the Fetal Mouse Mammary Gland

Laura N. Vandenberg, Maricel V. Maffini, Perinaaz R. Wadia, Carlos Sonnenschein, Beverly S. Rubin, and Ana M. Soto

Department of Anatomy and Cellular Biology, Tufts University School of Medicine, Boston, Massachusetts 02111

Abstract

Humans are routinely exposed to bisphenol-A (BPA), an estrogenic compound that leaches from dental materials, food and beverage containers, and other plastic consumer products. Effects of perinatal BPA exposure on the mouse mammary gland have been observed in puberty and adulthood, long after the period of exposure has ended. The aim of this study was to examine fetal mammary gland development at embryonic day (E)18 and assess changes in the tissue organization and histoarchitecture after exposure to an environmentally relevant dose of BPA. In unexposed fetuses, the relative position of the fetus with respect to its female and male siblings in the uterus influenced growth of the ductal tree, which was more developed in females placed between two males than in females placed between two females. Exposure of dams to 250 ng BPA per kilogram body weight per day from E8 to E18 significantly increased ductal area and ductal extension in exposed fetuses and obliterated positional differences. In the stroma, BPA exposure promoted maturation of the fat pad and altered the localization of collagen. Within the epithelium, BPA exposure led to a decrease in cell size and delayed lumen formation. Because mammary gland development is dependent on reciprocal interactions between these compartments, the advanced maturation of the fat pad and changes in the extracellular matrix may be responsible for the altered growth, cell size, and lumen formation observed in the epithelium. These results suggest that alterations in mammary gland phenotypes observed at puberty and adulthood in perinatally exposed mice have their origins in fetal development.

Epidemiological studies and animal experimentation have revealed that alterations in the nutritional status of a developing fetus may increase susceptibility to disease later in life (1, 2). This new emphasis on the fetal origin of adult disease, in combination with epidemiological data, has prompted scientists to hypothesize that prenatal exposure to synthetic estrogen-like chemicals, *i.e.* xenoestrogens, may play a role in the increased incidence of breast cancer over the last 50 yr (3–5).

Bisphenol-A (BPA), a plasticizer used in the manufacturing of polycarbonate plastics and epoxy resins, has been shown to leach from food and beverage containers (6–8) and dental sealants and composites (9) under normal conditions of use (10). This xenoestrogen has been measured in maternal and fetal plasma and placental tissue at birth in humans (11,12). A recent study of 394 Americans reported that BPA was found in 95% of urine samples (13). From

Address all correspondence and requests for reprints to: Ana M. Soto, Tufts University School of Medicine, Department of Anatomy and Cellular Biology, 136 Harrison Avenue, Boston, Massachusetts 02111. ana.soto@tufts.edu.

Disclosure statement: the authors have nothing to disclose.

these data, the mean exposure was estimated to be 40 ng/kg body weight (BW) per day and the 95th percentile was 230 ng/kg BW per day, assuming that 70% of the daily dose was excreted into the urine. A smaller study estimated a maximum daily intake of BPA to be 230 ng/kg BW (14).

Exposure of rodents to low doses of BPA during fetal development has been shown to induce early vaginal opening (15), advance the onset of puberty (16), disrupt estrous cyclicity (17, 18), and decrease serum levels of LH after ovariectomy (18). Perinatal exposure to BPA alters postnatal mammary gland development (3,4) and increases the sensitivity to estradiol at puberty (4). We postulate that these changes are a consequence of altered development during the period of BPA exposure.

Like other ectodermal appendages such as teeth, hair, and salivary glands, the fetal mammary gland is formed by reciprocal interactions between multiple tissue compartments. The mammary epithelium, derived from the embryonic ectoderm, and the mammary mesenchyme, derived from the embryonic mesoderm, are first detected between embryonic day (E)10 and E11 in the mouse (19). From E11 to E12.5, the epithelial placodes begin to increase in size to form rounded buds, and estrogen receptor (ER)- α and ER β mRNAs begin to be expressed in the mesenchyme (20). Between E13 and E15, the epithelial buds invaginate into the underlying mesenchymal tissue, which becomes denser in the area abutting the mammary epithelium (21). Finally, on E16, the epithelium forms a primary sprout, which undergoes a significant increase in proliferation before it pushes through the closely associated mammary mesenchyme and penetrates the primitive fat pad, a cluster of preadipocytes found in the deeper dermal tissue (21). Several days later, the mammary epithelium branches and the epithelial cord hollows to allow for the formation of a continuous lumen (22).

We chose to examine the hypothesis that BPA alters fetal mammary gland development at E18, a time during which ductal branching and fat pad differentiation are taking place, thus providing various measurable morphological end points that could be potentially altered by BPA exposure. Based on available information (13,14), we chose to expose dams to 250 ng BPA/kg BW·d, a dose that should fall within the range of estimated human exposure. We began by observing the normal morphology of the mammary gland at E18, a time point that has not been extensively described before this study, and found that exposure to BPA altered several of the growth parameters measured. Because mammary gland development is dependent on reciprocal interactions between the stroma and the epithelium, we also studied the morphological and histological characteristics of both compartments.

Materials and Methods

Dosing of dams with BPA

Sexually mature female CD-1 mice (8 wk of age; Charles River Laboratories, Wilmington, MA) were maintained in temperature-controlled and light-controlled (14-h light, 10-h dark cycle) conditions in the Tufts University School of Medicine animal facility. All experimental procedures were approved by the Tufts University-New England Medical Center Animal Research Committee in accordance with the Guide for Care and Use of Laboratory Animals. Cages and bedding tested negligible for estrogenicity by the E-SCREEN assay (23); water was supplied from glass bottles only. Food (Harlan Teklad 2008; Indianapolis, IN) was supplied *ad libitum*; estrogenicity of feed was measured at 20 fmol of estrogen equivalents per gram, a negligible amount (23). Female mice were mated with CD-1 breeding males, and the morning on which a vaginal plug was observed was designated E1. On the evening of E8, mice were weighed and implanted with Alzet osmotic pumps (Alza Corp., Palo Alto, CA) designed to deliver either 50% dimethyl sulfoxide (vehicle control) or 250 ng BPA per kilogram BW per day dissolved in vehicle. The actual delivered dose decreased as pregnancy progressed because

the weight of the mother increased over this period. This dose was chosen both because it is thought to be environmentally relevant and it has been shown to alter more end points than the lower doses in our previous studies, in both the mammary gland (3,4,17) and other estrogen-target organs (24,25).

Delivery and dissections

On the afternoon of E18, dams were injected with a sublethal dose of ketamine and xylazine, and fetuses were delivered singly by cesarean section and decapitated. The position of each fetus in the uterus was recorded and the fourth inguinal mammary glands were dissected from each female with the aid of a dissection microscope (Zeiss, New York, NY). Briefly, an incision was made through the skin from the vagina to the neck. The skin was gently peeled away from the muscle wall of the body, and the mammary gland was removed from the skin. One mammary gland was whole mounted and its contralateral gland was embedded in paraffin for light microscopy and immunohistochemical analysis. Additional fourth inguinal mammary glands were collected in RNase-free conditions for RT-PCR analysis. These glands were immediately immersed in RNA-later (Ambion, Austin, TX) and stored at 4 C after the completion of the dissections. Glands were then transferred to RNase-free Eppendorf tubes and stored at -80 C.

Whole mounts and paraffin embedding

To prepare the whole mounts, the mammary glands were spread onto glass slides, fixed with 4% paraformaldehyde (Polysciences, Warrington, PA) in 0.1 M PBS overnight, stained with Carmine Alum (Sigma, St. Louis, MO), dehydrated, and mounted with Permount (Sigma). To prepare paraffin sections, mammary glands were fixed with 4% paraformaldehyde in 0.1 M PBS for 18–20 h at room temperature, washed in 0.1 M PBS, dehydrated through a series of alcohols and xylene, and embedded with Paraplast paraffin (Fisher, Fair Lawn, NJ) under vacuum. Five-micrometer sections were cut on an RM2155 rotary microtome (Leica, Québec, Canada) and mounted on Superfrost slides (Fisher); the entire mammary gland was sectioned at once. Sections were processed through xylenes to remove the paraffin, and hydrated by a series of alcohols. Every fifth section was stained with Harris' hematoxylin to determine the presence of epithelial cords; only those sections with visible cords were used for further analysis. Epithelial cords were examined in each section for the initiation of lumen formation indicated by the absence of cells in the inner part of the cord.

Immunohistochemistry

Sections were treated with xylene to remove paraffin and rehydrated through a series of alcohols and PBS and then microwaved in 10 mM citrate buffer (pH 6) for antigen retrieval. Nonspecific binding was blocked for 1 h with normal goat serum in 1.5% milk. Sections were incubated overnight at 4 C in a humid chamber with primary antibody. Biotinylated goat antirabbit IgG (Zymed, San Francisco, CA) was applied to sections for 1 h in a humidified chamber at room temperature. Slides were rinsed with PBS and detection of positive cells was accomplished using alkaline phosphatase (Vectastain ABC-AP kit; Vector, Burlingame, CA) or streptavidin-peroxidase-diaminobenzidine (Sigma). Samples were counterstained with Harris' hematoxylin, dehydrated, and mounted with a permanent mounting medium. Immunohistochemistry was performed for Ki67 (Vector), a nuclear antigen expressed by proliferating cells; Bax (Santa Cruz Biotechnology, Santa Cruz, CA), a positive regulator of apoptosis; adipocyte lipid binding protein (ALBP) (Abcam, Cambridge, UK), a protein that binds long-chain fatty acids found in adipocytes and adipocyte precursors; and ER α (Abcam). Primary and secondary antibody concentrations were as follows: Ki67, 1:5000/1:2000; Bax, 1:100/1:500; ALBP, 1:200/1:500; ER α , 1:500/1:1000.

Morphometric and thresholding analysis

Whole mounts—Whole mounted mammary glands were viewed through a Zeiss Stemi 2000-c dissection scope at $\times 3.2$. Images were captured by an AxioCam HRC digital camera (Zeiss) at 2600 dots per inch (dpi) and processed with Axiovision software (version 4.3; Zeiss) to measure the following parameters: area of the ductal tree, measured by outlining the ducts; area subtended by the ductal tree, measured by connecting the outermost edges of the ductal tree; ductal extension, measured as the distance from the nipple to the furthest point of growth; number of branching points; number of secondary and tertiary branches; number of terminal ends; and primary duct length, measured as the distance from the nipple to the first branching point.

Sections stained with hematoxylin—Sections were viewed through a Zeiss Axioskop 2 plus light microscope at $\times 5$ and $\times 10$. Images were captured at 3900 dpi using the AxioCam HRC digital camera. Epithelial cords were examined in each section for lumen formation and morphological criteria were used to determine the percentage of epithelial cells that were apoptotic (26). In those sections in which no lumen was present, the total area covered by epithelium was measured using the Axiovision software and the number of cells within this area was counted; the average cell size was calculated from these measurements. In the stromal compartment, the location of each cell containing a clear vacuole was marked; the number of marked cells within discrete distances from the epithelium was measured. Additionally, fifteen $50 \times 50 \mu\text{m}$ boxes were randomly placed on cross-sections of each mammary gland. Within boxes that fell on the developing fat pad, the numbers of nuclei within the box were counted; the values for each box were averaged to obtain the fat pad cellular density.

Sections stained with Masson's Trichrome—To examine fibrous collagen, $5\text{-}\mu\text{m}$ sections stained with Masson's Trichrome were viewed and images captured as described for hematoxylin. Using the Axiovision software, the density and relative area covered by each compartment was measured. Morphometric analysis used $20 \times 20 \mu\text{m}$ grids placed on five random fields to assess the number of vacuoles and size of vacuoles per adipocyte. Additionally, thresholding techniques were used to compare the area covered by collagen and the density of collagen within defined regions. Briefly, a baseline threshold for intensity of blue (collagen) staining was selected blindly. The Axiovision program then determined the amount and density of collagen in each sample at or above that threshold. Area occupied by collagen and density of collagen staining was measured in entire sections or in regions within 10, 20, 30, and $50 \mu\text{m}$ of the epithelium.

Epithelial immunohistochemistry—Five-micrometer sections were viewed and captured as described for hematoxylin. For Ki67 and Bax immunohistochemistry, both positive cells and total cells in the epithelial compartment were counted; percentage of positive cells were calculated. Positive cells were also separated by their location in the epithelial cord. Cells along the outer edge of the epithelium were considered outer cord cells and cells on the inner portion of the epithelium were considered inner cord cells. For ER α immunohistochemistry, qualitative observations were made regarding the location and type of staining (cytoplasmic or nuclear).

Stromal immunohistochemistry—Bax and ER α expression were each observed in $5\text{-}\mu\text{m}$ sections viewed and captured at $\times 10$ and 3900 dpi. For each sample, five image fields were captured. Using morphometric analysis techniques as described by Howard and Reed (27), a $25 \times 25 \mu\text{m}$ grid was placed on each field. Positive cells were counted only when they were located at the cross-hairs of the grid, allowing us to determine the volume fraction occupied by positive cells. Each cell was further classified by its location in the connective tissue or the developing fat pad. For ALBP immunohistochemistry, qualitative observations were made regarding the cellular localization of the staining and type of cells stained.

RNA isolation and quantitative real-time RT-PCR

RNA isolation and quantitative RT-PCR protocols were followed as described previously (4) using mammary glands pooled from all female pups in a litter. The PCR program was 95 C for 15 min for activation of the *Taq* polymerase followed by 45 cycles of 95 C for 15 sec, 59 C for 30 sec, and 72 C for 30 sec. A dissociation curve was set up at the end of the run to determine the purity of the PCR products.

Forward and reverse primers were as follows: ER α forward, ttgatcaaggcagtcacaa, reverse, ctccgagtcacagtcattgc (detecting nucleotides 2886–3000); peroxisomal proliferator-activated receptor (PPAR)- γ forward, aggccgagaaggagaagctgttg, reverse, tggccacctttgctctgctc (detecting nucleotides 683–958); ER β forward, tggcaagcttgatgtgac, reverse, tgacagtgaccacattcagaca (detecting nucleotides 2570–2673); ALBP forward, ctggtgcaggtgcagaagt, reverse, aatttccatccaggctctt (detecting nucleotides 317–470); collagen I forward, gtcctagtcgatggctgctc, reverse, acacggaattctggtcagc (detecting nucleotides 4034–4173 of procollagen type1 α 2); L19 (housekeeping gene) forward, atcccaatccaactcc, reverse, tcaccttctcaccagtgca (detecting nucleotides 101–305).

A pubertal mammary gland was included in every run as a positive control and identified as the calibrator. The cycle threshold values of the gene of interest for each sample were first normalized to the housekeeping gene (L19). The fold change of gene expression for every sample was then calculated with respect to the calibrator sample.

Statistics

The SPSS statistical software package 10.1 (SPSS Inc., Chicago, IL) was used for all statistical analysis; *t* tests were used to directly compare vehicle and BPA-treated whole mounts. ANOVA tests were used to assess differences between each uterine positioning group and planned *t* tests were used to compare control and 250 ng/kg BW-d BPA groups at each uterine position. Because no histological or immunohistological end points were found to be influenced by intrauterine positioning, a single fetus from each litter, chosen arbitrarily with respect to intrauterine position, was used for further analyses.

Because the data were not normally distributed, we used Mann-Whitney *U* nonparametric tests to compare control and BPA-exposed groups for histological studies. Because individual offspring cannot be exposed prenatally, we were obliged to dose the dams. Hence, we were careful to randomize maternal effects and maximize the number of maternal units represented in each group. For each histological measurement, only one individual from a given litter was assigned to each group or end point. Finally, a χ^2 test was performed to compare the incidence of lumen in the mammary gland epithelium of control and BPA-exposed animals. For all statistical tests, results were considered significant at $P < 0.05$. All results are presented as mean \pm SEM.

Results

Morphological parameters of the fetal mammary gland

We performed morphometric analysis of mammary gland whole mounts for several parameters including ductal area, maximal width of the ductal tree, length of the primary duct, farthest extension of the ductal tree, number of branching points, number of tertiary branches, and number of terminal ends (Fig. 1A). The overall size of the vehicle-treated ductal tree varied widely among subjects, with ductal area ranging from 0.03 to 0.15 mm² and the area subtended by the ductal tree ranging from 0.07 to 0.40 mm² (Table 1). We also measured ductal extension, and found less variation in this parameter (0.48–1.10 mm). Additionally, we found a great

variety in the number of branching points (range 1–7) and its related parameter, the number of terminal ends (range 2–8).

BPA alters the overall organization of the fetal mammary gland

When we compared the morphological characteristics described above for the vehicle-exposed mice with BPA-treated animals, we found that overall, the BPA-exposed animals were more developed for each morphological parameter (Fig. 1B); significant differences between these two groups were observed for absolute ductal area ($P = 0.043$) and ductal extension ($P = 0.008$) (see Table 1).

Normal mammary gland development is affected by intrauterine position

vom Saal and colleagues (28,29) observed effects in mice of several endocrine-related end points that were attributed to the localization of the fetus in the uterus with respect to the sex of the fetuses in close proximity. These effects are often referred to as intrauterine positioning effects (see Ref. 30 for a comprehensive review). Because of the wide range of variation in the parameters measured in E18 whole mounts, we ranked each mammary gland according to the relative position of the fetus with respect to its female and male siblings in the uterus. Several growth parameters in the ductal tree appeared to be influenced by the intrauterine position of the fetus. For instance, females positioned between two females [0 male (0M) females] had fewer branching points (Fig. 1C) and fewer terminal ends (data not shown) than females positioned between 1 male and 1 female (1M females) ($P = 0.022$ and $P = 0.053$, respectively) as well as females positioned between two males (2M females) ($P = 0.027$ and $P = 0.041$, respectively). We found that the area subtended by the ductal tree was significantly smaller in 0M females, compared with 2M females ($P = 0.043$) (Fig. 1D); additionally, the ductal extension of 0M females was shorter than in 2M females (Fig. 1E), although this trend was not statistically significant ($P = 0.057$).

BPA alters mammary gland patterning induced by intrauterine position

We examined the morphological characteristics of BPA-exposed mammary glands taking into consideration the intrauterine positioning of each fetus. Whereas in control mammary glands we found that 0M females had significantly fewer branching points and terminal ends than 1M or 2M females, in BPA-exposed animals, this pattern was obliterated. In fact, we observed that 0M females exposed to BPA had a significant increase in branching points, compared with control 0M females ($P = 0.042$) (Fig. 1C). We also found that in control animals, the area subtended by epithelial ducts was affected by intrauterine positioning; interestingly, this position-specific effect was not present in BPA-exposed animals (Fig. 1D). Finally, exposure to BPA caused an increase in ductal extension in 1M and 2M females, compared with their control counterparts (Fig. 1E), which was statistically significant in the 1M females ($P = 0.026$).

Epithelial cell characteristics and lumen formation

We began by examining the morphological characteristics of the epithelial cells in the mammary gland. In general, the epithelial cells were rounded or oval-shaped (Fig. 2A). The cells along the outer border of the epithelial cord seemed to be arranged in a tight manner, whereas the cells toward the inner portion of the epithelial cord were more heterogeneous in size and shape. Most glands appeared to have a large amount of space between cord cells, and the cells were arranged irregularly within the epithelial cord. Based on these morphological criteria, we separated the epithelium into outer cord cells, comprised of the outermost layer of epithelium directly in contact with the basement membrane, and inner cord cells, comprised of all inner layers not in direct contact with the basement membrane. We also examined the expression of Ki67 to assess proliferation in the epithelial cords (Fig. 2C). We noted that 2.58

$\pm 0.69\%$ of epithelial cells expressed Ki67, and these cells were equally abundant in the outer ($1.37 \pm 0.59\%$) and inner cord cells ($1.21 \pm 0.35\%$) (Fig. 2D).

Every fifth section containing epithelial ducts was examined in depth. Some of the sections had epithelium with a very distinct absence of cells in the region in which the inner cord cells were normally present. We considered this distinct absence of inner cord cells to be the developing lumen (Fig. 2E). Because the fetal gland forms as a solid cord of epithelium but the adult ducts consist of hollow tubes, it was expected that the inner cord cells would either be relocated within the compartment or undergo programmed cell death (19). To determine whether apoptosis was playing a role in lumen formation, immunohistochemistry was performed to localize Bax, a proapoptotic marker. We observed that $2.71 \pm 0.48\%$ of all cells in the epithelial cord were positive for Bax. However, the majority of the positive cells were located within the inner cord cells, and very few outer cells were immunoreactive (Fig. 2G), indicating that the formation of a lumen is likely to be dependent on cell death in the inner cord cells.

BPA alters the mammary gland epithelium

Unlike the rounded epithelial cells in control mammary glands, we found the epithelium of BPA-exposed animals to be more spindle shaped and evenly spaced within the confines of the epithelial cord. Additionally, we observed that the average number of cells per unit area of epithelium was significantly increased in BPA-exposed compared with control animals, indicating that the epithelium is tightly compacted and the average cell size is smaller in the epithelium of BPA-exposed animals (control, $55.07 \pm 2.02 \mu\text{m}^2$; BPA, $50.63 \pm 2.62 \mu\text{m}^2$; $P = 0.007$; $n = 7$) (Fig. 2B). We also examined the overall expression and localization of Ki67 within the epithelial compartment. There were no statistically significant differences in Ki67 expression in BPA-exposed mammary glands compared with controls (Fig. 2D).

In vehicle-exposed animals, we found that six of the 16 animals examined had a clear lumen present. Of 10 BPA-exposed animals, none had a lumen present ($P = 0.035$), indicating that lumen formation may be delayed in these animals (Fig. 2F). We also examined the expression of Bax in the epithelium of BPA-exposed females. When the Bax-positive cells were separated based on their location in the epithelium (outer vs. inner cord cells), a significant decrease in Bax-positive cells was observed in the inner cord cells of BPA-exposed relative to control mammary glands (control: $2.14 \pm 0.39\%$, BPA: $0.80 \pm 0.11\%$, $P = 0.021$), whereas there were no differences in Bax-positive cells in the outer cells of the BPA-exposed and control glands (control: $0.58 \pm 0.14\%$, BPA: $1.05 \pm 0.44\%$, $P = 0.309$) (Fig. 2G). Similar results were obtained using morphological criteria for apoptotic cells (data not shown). The decrease in apoptotic cells in the central portion of the mammary gland epithelium may explain the absence of lumen formation observed in the BPA-treated animals, compared with controls.

Development of the stromal compartment

Sections stained with hematoxylin illustrated the heterogeneity of the mammary gland stroma, comprised mostly of loosely connected rounded and fibroblast-like cells scattered within abundant matrix. Interspersed within this tissue were several dozen clumps of closely associated cells. These clumps varied in size and had irregular shapes. To further characterize the compartments of the mammary stroma, we stained mammary gland sections with Masson's Trichrome (Fig. 3A). Thus, we were able to easily differentiate among the epithelium, connective tissue, blood vessels, lymph node, and developing fat pad.

Areas of the stroma having sparse cellular contributions were identified as loose connective tissue regions. The developing fat pad was characterized by clumps of cells, many of which had visible, clear vacuoles (Fig. 3C). We measured the area occupied by each compartment

within the tissue sections relative to the area of the entire section and found that $81.4 \pm 2.3\%$ of the gland was comprised of loose connective tissue and $16.9 \pm 2.2\%$ was the fat pad (Fig. 3D). The remainder of the area was occupied by the lymph node, blood vessels, and epithelial cord.

To determine whether the cells containing clear, unstained vacuoles were adipocytes or preadipocytes, we stained mammary gland sections with antibodies against ALBP, a protein found in both cell types. These cells demonstrated positive staining in both the cytoplasmic and nuclear compartments (Fig. 3E). The localization of ALBP to both cellular compartments and the rounded, lobular appearance of these cells indicates that they are either committed preadipocytes or differentiated adipocytes (31).

BPA alters the developing fat pad

The relative areas covered by each stromal compartment in the mammary gland were unchanged after BPA treatment (loose connective tissue: $77.2 \pm 3\%$, fat pad: $20.8 \pm 2.7\%$) (Fig. 3D). The area covered by blood vessels and the lymph node were also unaffected by treatment, and no gross changes in these structures were noted.

When we assessed the OD of each compartment, we observed a significant decrease in the density of the fat pad of BPA-exposed relative to control mammary glands ($P = 0.004$) (Figs. 3B and 4A). We hypothesized that this decrease in OD was due to either a decrease in the total number of cells or an increase in the amount of fat-containing vacuoles stored in the cytoplasm of these cells.

To determine whether this decrease in OD was due to a decreased number of cells in the developing fat pad, we measured the number of cells in this compartment. This morphometric analysis revealed that, in fact, the fat pads of BPA-exposed animals are significantly less cellular than the fat pads of control animals (control, 38.39 ± 1.92 ; BPA, 32.57 ± 1.05 ; $P = 0.033$). Additionally, to determine whether BPA exposure caused alterations in apoptosis in the mammary fat pad, we performed immunohistochemistry for Bax. A significant increase in Bax-positive cells was noted in the developing fat pad of BPA-exposed mammary glands ($P = 0.047$) (Fig. 4B). These results suggest that apoptosis may be playing a role in the decreased cellular density of the developing fat pad of BPA-exposed females.

To determine whether the decreased OD of the developing fat pad in BPA-exposed animals was also due to an increase in the number of cells with unstained fat vacuoles, we counted the number of cells with clear inclusions in the cytoplasm. The total number of cells with vacuoles was increased in the fat pad of BPA-exposed animals, although this increase was not statistically significant ($P = 0.076$) (Fig. 4C). However, the pattern of localization of these cells was significantly altered after BPA exposure. When we measured the number of cells with clear inclusions within several distances from the epithelial compartment, there were significantly more cells with fat vacuoles in the BPA-exposed mammary glands, compared with controls at distances less than 1 mm ($P < 0.02$) (Fig. 4D). The altered localization/patterning was significant, even at distances less than $75 \mu\text{m}$ from the epithelium ($P = 0.011$). These data suggest that the epithelium of BPA-exposed animals is penetrating the fat pad to a greater degree than the epithelium of control animals and may also indicate an advanced maturation of the cells comprising the fat pad. Additional examinations of cells within the fat pad indicate that BPA treatment may be altering development of adipocytes. The average cell in the fat pad of BPA-exposed mammary glands had significantly more vacuoles, compared with controls (control: 1.512 ± 0.057 , BPA: 1.777 ± 0.037 , $P = 0.004$). However, the size of the individual vacuoles was not affected by BPA treatment (control: $12.51 \pm 0.973 \mu\text{m}^2$, BPA: $12.94 \pm 1.506 \mu\text{m}^2$). Additionally, expression of PPAR γ , a marker for adipocyte differentiation, did not show any differences based on treatment (Table 2). However, expression of ALBP

mRNA was increased in the BPA-exposed mammary glands, compared with controls, although this increase was not statistically significant (Table 2).

Collagen localization

The use of Masson's Trichrome stain allows for the localization of collagen in the mammary gland stroma. In most of the glands examined, this collagen was stained a dark blue and was abundant. Most of the collagen was distributed through the loose connective tissue regions, between the patches of the developing fat pad (Fig. 3A). There was also a small layer of collagen directly abutting the epithelial cords; we referred to this collagen as periductal (Fig. 5A).

BPA alters collagen localization

Sections stained with Masson's Trichrome indicated differences in collagen localization in BPA-exposed mammary glands when compared with controls (Fig. 3, A and B). Overall, both the density of collagen deposits (Fig. 5C) and area covered by collagen were decreased in BPA-exposed glands ($P = 0.014$ and $P = 0.025$, respectively). We also examined the periductal collagen in BPA-exposed glands (Fig. 5B). The density of collagen within $10 \mu\text{m}$ of the epithelium, within the first layer of stromal cells, was significantly increased in BPA-exposed glands, compared with controls ($P = 0.042$) (Fig. 5D). These differences were no longer present at 20, 30, or $50 \mu\text{m}$ from the epithelium. Expression of collagen type I mRNA was not different in the BPA-exposed and control glands (Table 2), likely because this method used mRNA from the entire mammary gland, which is heterogeneous.

ER expression

ER α and *ER β* mRNAs have previously been detected in mammary glands from E12.5 to E14. These transcripts are primarily localized to the developing periepithelial mesenchyme (20). Autoradiographic experiments also revealed specific ^3H -diethylstilbestrol binding in the mesenchyme surrounding the epithelium at E16, suggesting the presence of functional receptor in this region (32). We used RT-PCR to determine whether the mRNAs for *ER α* and *ER β* are still present at E18 and observed that, in fact, transcripts for both receptors are present in the E18 mammary gland (Table 2). In addition, immunohistochemical analysis revealed that *ER α* -positive cells were present in the loose connective tissue and fat pad compartments of the developing stroma (Fig. 6A) and the developing blood vessels. Punctate staining was observed in the nucleus and cytoplasm of some mammary epithelial cells (Fig. 6B), whereas others were completely negative. Negative control slides (incubated without primary antibody) were free of staining in either compartment (Fig. 6C).

ER localization in the mammary glands of BPA-exposed animals

There were no statistically significant differences in *ER α* or *ER β* mRNA expression between BPA-exposed animals relative to controls (Table 2) or by quantification of ER-positive cells by immunohistochemistry (relative volume fraction of positive cells: vehicle, 0.78 ± 0.21 ; BPA, 1.13 ± 0.27). Further analysis revealed no statistically significant differences in the distribution of *ER α* -positive cells in either the connective tissue or the fat pad. Additionally, we also noted expression of *ER α* in the epithelial compartment of BPA-exposed females, often as a punctate staining in only a small region of the cord (data not shown). However, we did not observe any qualitative differences based on treatment.

Discussion

Female fetuses exposed *in utero* to 250 ng BPA per kilogram BW per day starting at E8 displayed an overall altered morphology of the mammary gland at E18 involving the epithelial ductal tree, loose connective tissue, and developing fat pad. These results suggest that BPA

exposure accelerates differentiation of the mammary fat pad, which in turn may facilitate the increased growth of the ductal tree. Additionally, BPA exposure induced changes in the extracellular matrix of the periductal stroma, which may, in turn, lead to the altered morphology observed in the epithelial cord cells, including the delay in lumen formation.

BPA induces epithelial growth, advances fat pad maturation, and alters collagen localization

BPA treatment increased ductal growth at E18, both in area and extension. The number of Ki67-positive epithelial cells was not significantly increased at this time, arguing against active proliferation at E18. Moreover, the average epithelial cell size was significantly reduced in the BPA-treated animals, thus ruling out cell hypertrophy as the cause of increased ductal growth. Therefore, it is likely that a proliferative response to BPA occurred before E18.

In the mammary mesenchyme, the fat pad of BPA-exposed animals was significantly less dense relative to controls. This was likely due to the decrease in the number of cells per unit area, increase in apoptosis, and increase in the number of cells containing fat vacuoles. In addition, there was a significant increase in the number of adipocytes within 1 mm of the epithelial tree in the mammary gland of BPA exposed animals. These findings suggest that BPA exposure results in accelerated fat pad maturation, which in turn may induce ductal growth. This interpretation is supported by *in vivo* and *in vitro* studies that revealed interactions between adipocytes and epithelial cells and their influence on epithelial differentiation, growth and cell morphology (33–39).

In vitro studies have demonstrated that the mouse non-mammary preadipocyte cell line 3T3-L1 (33,34), excised mammary fat pads (35,36), and adipocytes isolated from the mammary gland (37) are capable of inducing proliferation and morphological differentiation of mammary epithelial cells. *In vivo* studies showed that mammary epithelium recombined with fat pad precursor cells form normal end buds and ductal outgrowths (38). In contrast, recombination of epithelium with fibrous mammary stroma led to the development of abnormal, compact epithelial structures. Additionally, branching of the ductal epithelium does not occur before E16, when the first sign of adipocyte differentiation is apparent in the mammary gland. These results suggest that ductal branching occurs at this developmental state due to the inductive properties of the fatty stroma (38). Moreover, studies of mice completely lacking white adipose tissue revealed that the mammary ducts cease to grow or branch after E18 (39), suggesting that at this point in development, the mammary epithelium is dependent on, and perhaps especially sensitive to, modulating signals from the surrounding fat pad. It is plausible that the increase in adipocytes we observed after BPA exposure could lead to a change in a morphogen or morphostat gradient, which would increase ductal growth in these animals.

An additional conclusion from the findings presented here is that BPA may increase the differentiation rate of adipocytes, thus explaining why a greater number of stromal cells containing fat vacuoles were present in BPA-exposed animals. *In vitro* studies have shown that BPA, in combination with insulin, can accelerate the differentiation of adipocytes from a fibroblast cell line (40). Our studies revealed the presence of more fat vacuoles per cell in BPA-exposed than control mammary glands suggesting that BPA accelerates lipid-uptake, a sign of advanced maturation of the fat pad.

BPA-exposed animals had a greater collagen density within 10 μm of the ductal epithelium, compared with controls. Studies in normal fetal mammary glands (41), transplantation experiments (42), and three-dimensional cell cultures (43) revealed that collagen influences the morphology of the mammary epithelium. Of particular importance in this regard have been three-dimensional cultures of epithelial cells with varying amounts of type I collagen. Epithelial cells grown in a matrix that resembles the collagen composition of the normal mammary gland demonstrated normal epithelial morphogenesis (43). However, even small

increases in collagen in the matrix surrounding the epithelial cells led to altered organization of the epithelial cells and inhibited lumen formation. Thus, the alterations we observed in epithelial cell size, lumen formation, and epithelial morphology may be due to modifications in the content of periductal collagen, which is most closely associated with the epithelial ducts.

Our results also indicate that in the overall stroma, both the area covered by collagen and its collagen density decreased after BPA exposure. This result suggests that BPA distinctly affects two different stromal cell populations, one adjacent to the epithelium and a second population in the loose connective tissue. In fact, it has been suggested that the fibrous connective tissue and the adipose tissue within the mammary gland produce different types of basement membrane and extracellular matrix (44). Therefore, it is plausible that the increased number of adipocytes in the mammary glands of BPA-exposed fetuses could alter the collagen content of the mammary stroma. Additionally, it is likely that BPA differentially alters collagen deposition or its degradation within these two regions of the stroma.

Does BPA act as an estrogen in the E18 mammary gland?

BPA is a full agonist that binds both ER α and ER β , although at lower affinities than estradiol (45,46). ER α and ER β mRNAs are both expressed in the mammary mesenchyme from E12.5 to E14 (20). In addition, autoradiographic experiments showed specific ³H-diethylstilbestrol binding at E16, suggesting the presence of functional receptors in the mesenchyme surrounding the epithelium (32). Moreover, we observed herein that ER α and ER β mRNAs are expressed in the E18 mammary gland. These data suggest that during the period of exposure we studied, ER is not only expressed but functional, and that BPA may be acting through the ERs. In fact, studies using a transgenic mouse line carrying a luciferase reporter construct coupled to estrogen response elements showed that BPA administered to these dams at E13.5 caused activation of ER in the developing fetuses within 8 h of exposure (47). More specifically, BPA may be targeting ER in the stromal compartment. Antibodies against the ER α protein showed that this receptor is present predominantly in the stromal compartment, but punctate expression is also apparent in the epithelium. Because ER α expression is thought to be confined primarily to the epithelium at postnatal time points (48), it is likely that at E18, there is a transition of primary ER expression from one compartment to the other. Therefore, whereas we reason that BPA acts through the stromal ER, we cannot rule out a direct action of BPA in the mammary epithelium at E18 and later. Reciprocal mammary gland recombinations would address this question directly. On the other hand, low-dose BPA effects may occur through an ER residing in the plasma membrane that binds xenoestrogens with a higher affinity than the nuclear ERs (49).

It is possible, albeit unlikely, that BPA is acting on the fetal mammary gland through a mechanism that does not involve ER. For instance, there is evidence that BPA binds to thyroid hormone receptor, although the affinity of BPA for this receptor is severalfold lower (50) than its affinity for the ERs (51). Additionally, *in vivo* effects of BPA on thyroid hormone signaling have been obtained at doses more than 10,000-fold higher than those examined in the current study (52). Moreover, there is no evidence to relate thyroid hormone receptor to embryonic mammary gland development. BPA has also been shown to have antiandrogenic activity, at doses several orders of magnitude higher than those used in the current study (53). Additional experiments involving receptor knockout animals may further elucidate the mechanisms responsible for BPA action.

Hormonal mediation of intrauterine positional effects

Our results revealed that normal mammary gland development is influenced by intrauterine position; the mammary glands of female fetuses located between two females in the uterus (0M females) were generally less developed than females positioned between two males (2M

females). This novel finding in the mammary gland positively correlates with previous reports of intrauterine positional effects on other endocrine-related end points such as prostate growth (54), responsiveness to testosterone (55), steroid metabolism (56), and age of pubertal onset and estrus cycle length (57). Our results show that some positional effects apparent in vehicle-treated litters are obliterated by treatment with BPA such that the mammary glands of 0M BPA-exposed females are more developed than those of their vehicle-treated counterparts and similar to those seen in 2M females exposed to either vehicle or BPA.

The actual mechanisms responsible for differences in development based on intrauterine position remain unknown. It was observed that 2M females have higher levels of testosterone in their serum and amniotic fluid (28) and are more masculinized than their 0M counterparts (58). This has been attributed to the diffusion of testosterone produced by the testes of neighboring males (59) (reviewed in Ref. 30).

Androgen receptor knockout females show impaired mammary ductal growth in postnatal life (60), suggesting that androgens may play an important role in postnatal gland development. If intrauterine positional effects are truly established by testosterone, one might conclude that 0M females have less developed mammary glands due to lower levels of testosterone. However, there are two potential problems with this conclusion: first, fetal testosterone exposure induces apoptosis of the epithelial stalk (61); and second, BPA is not thought to have androgenic activity at these low doses (53,62) and therefore should not obliterate positional effects through this pathway. However, it is known that androgen metabolites can bind to ER and produce estrogenlike effects (63). Additionally, it is possible that testosterone from neighboring male fetuses is being aromatized to estrogen in the fat of developing 2M mammary glands because fat elsewhere in the body is known to have aromatase p450 activity (reviewed in Ref. 64). Therefore, if local aromatization of testosterone can occur in the female fetus, 2M females would actually be exposed to greater levels of estrogen than 0M females, and BPA, acting as an estrogen, could obliterate positional differences as we have observed.

Additional studies have suggested that 0M females may have higher levels of estradiol in their serum and amniotic fluid than 2M females (65). However, because the fetal ovary is thought to be quiescent until several days after birth (66,67), the causal role of estrogen in positional effects is speculative at best because its origin in the fetus remains unclear. It is possible that the estradiol measured in fetuses originates from the dam and is bound to alpha-fetoprotein, a protein produced by the fetal liver that binds estrogens in the serum and amniotic fluid, thus making it unavailable to the developing fetus (68).

Consequences of xenoestrogen exposure during fetal life

Development of the fetal genital tract and mammary gland is affected by very low doses of BPA, whereas doses several orders of magnitude greater are required to evoke a uterotropic response in the prepubescent animal (69). Bern (70) proposed that the fetus is more susceptible to exogenous hormones than the adult due to irreversible effects that occur when organogenesis is affected. Our results indeed fit well within his proposal. BPA exposure during fetal development alters the normal morphogenesis of the mammary gland. These observations made in the mammary gland at E18 are likely to represent the primary events leading to the altered tissue organization that has been observed previously in BPA-exposed animals. However, we cannot rule out important effects of BPA on the mammary gland from E18 through postnatal d 2, a period during which developing animals in our previous studies continued to be exposed to BPA via the osmotic pumps implanted in their mothers. In fact, additional ductal branching and lumen formation does occur in the mammary gland from E18 until birth, and these events may also be compromised or altered by BPA exposure and could contribute to the mammary gland phenotypes we have observed at puberty and in adulthood. The observed alterations in mammary gland tissue organization together with an increased

sensitivity to estradiol are equivalent to human risk factors for breast cancer (4). These findings strengthen the hypothesis that exposure to xenoestrogens during early development may be an underlying cause of the increased incidence of breast cancer observed in European and U.S. human populations over the last 50 yr (3–5).

Acknowledgments

The authors are grateful to Cheryl Schaeberle for expert technical assistance and helpful suggestions on this manuscript and Dr. David Damassa for his assistance with statistical analysis.

This work was supported by National Institute of Environmental Health Sciences Grant ES08314 and a Tufts University Sackler Dean's Fellowship (to L.N.V.).

References

1. Barker DJP. The developmental origins of adult disease. *Eur J Endocrinol* 2003;18:733–736.
2. Godfrey KM, Barker DJP. Fetal programming and adult health. *Public Health Nutr* 2001;4:611–624. [PubMed: 11683554]
3. Markey CM, Luque EH, Munoz de Toro MM, Sonnenschein C, Soto AM. In utero exposure to bisphenol A alters the development and tissue organization of the mouse mammary gland. *Biol Reprod* 2001;65:1215–1223. [PubMed: 11566746]
4. Munoz de Toro MM, Markey CM, Wadia PR, Luque EH, Rubin BS, Sonnenschein C, Soto AM. Perinatal exposure to Bisphenol A alters peripubertal mammary gland development in mice. *Endocrinology* 2005;146:4138–4147. [PubMed: 15919749]
5. Durando M, Kass L, Piva J, Sonnenschein C, Soto AM, Luque EH, Munoz de Toro MM. Prenatal bisphenol A exposure induces preneoplastic lesions in the mammary gland in Wistar rats. *Environ Health Perspect*. 2006;110:1289/ehp.9282
6. Brotons JA, Olea-Serrano MF, Villalobos M, Olea N. Xenoestrogens released from lacquer coating in food cans. *Environ Health Perspect* 1994;103:608–612. [PubMed: 7556016]
7. Biles JE, McNeal TP, Begley TH, Hollifield HC. Determination of Bisphenol-A in reusable polycarbonate food-contact plastics and migration to food simulating liquids. *J Agric Food Chem* 1997;45:3541–3544.
8. Markey, CM.; Michaelson, CL.; Sonnenschein, C.; Soto, AM. Alkylphenols and bisphenol A as environmental estrogens. In: Metzler, M., editor. *The handbook of environmental chemistry*. Vol. 3. Part L, Endocrine disruptors, part I. Berlin Heidelberg: Springer Verlag; 2001. p. 129-153.
9. Olea N, Pulgar R, Perez P, Olea-Serrano F, Rivas A, Novillo-Fertrell A, Pedraza V, Soto AM, Sonnenschein C. Estrogenicity of resin-based composites and sealants used in dentistry. *Environ Health Perspect* 1996;104:298–305. [PubMed: 8919768]
10. Markey CM, Rubin BS, Soto AM, Sonnenschein C. Endocrine disruptors from Wingspread to environmental developmental biology. *J Steroid Biochem Mol Biol* 2003;83:235–244. [PubMed: 12650721]
11. Schonfelder G, Wittfoht W, Hopp H, Talsness CE, Paul M, Chahoud I. Parent bisphenol A accumulation in the human maternal-fetal-placental unit. *Environ Health Perspect* 2002;110:A703–A707. [PubMed: 12417499]
12. Ikezuki Y, Tsutsumi O, Takai Y, Kamei Y, Taketani Y. Determination of bisphenol A concentrations in human biological fluids reveals significant early prenatal exposure. *Hum Reprod* 2002;17:2839–2841. [PubMed: 12407035]
13. Calafat AM, Kuklennyik Z, Reidy JA, Caudill SP, Ekong J, Needham JL. Urinary concentrations of bisphenol A and 4-nonylphenol in a human reference population. *Environ Health Perspect* 2005;113:391–395. [PubMed: 15811827]
14. Arakawa C, Fujimaki K, Yoshinaga J, Imai H, Serizawa S, Shiraishi H. Daily urinary excretion of bisphenol A. *Environ Health Prev Med* 2004;9:22–26.
15. Honma S, Suzuki A, Buchanan DL, Katsu Y, Watanabe H, Iguchi T. Low dose effects of in utero exposure to bisphenol A and diethylstilbestrol on female mouse reproduction. *Reprod Toxicol* 2002;16:117–122. [PubMed: 11955942]

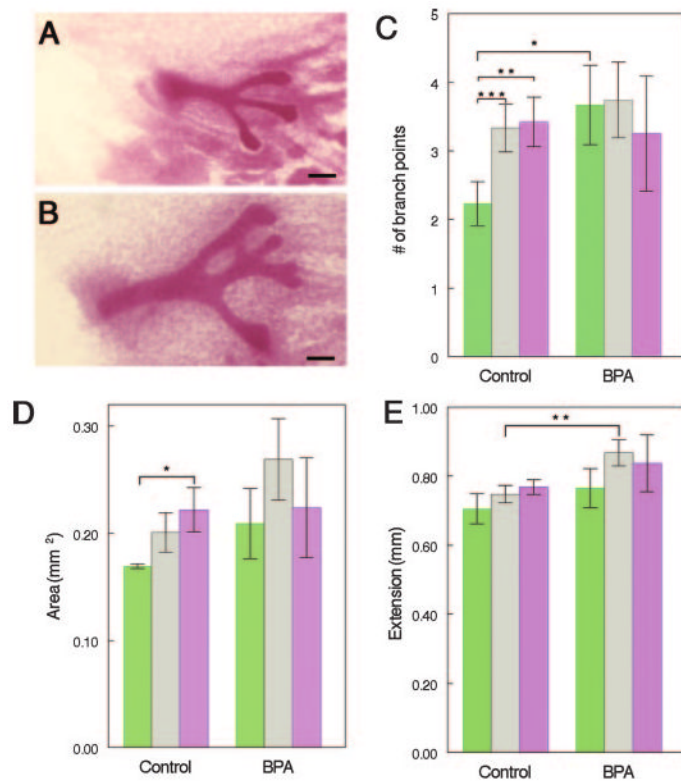
16. Howdeshell KL, Hotchkiss AK, Thayer KA, Vandenberg JG, vom Saal FS. Exposure to bisphenol A advances puberty. *Nature* 1999;401:763–764. [PubMed: 10548101]
17. Markey CM, Coombs MA, Sonnenschein C, Soto AM. Mammalian development in a changing environment: exposure to endocrine disruptors reveals the developmental plasticity of steroid-hormone target organs. *Evol Dev* 2003;5:1–9. [PubMed: 12492402]
18. Rubin BS, Murray MK, Damassa DA, King JC, Soto AM. Perinatal exposure to low doses of bisphenol-A affects body weight, patterns of estrous cyclicity and plasma LH levels. *Environ Health Perspect* 2001;109:675–680. [PubMed: 11485865]
19. Veltmaat JM, Mailloux AA, Thiery JP, Bellusci S. Mouse embryonic mammogenesis as a model for the molecular regulation of pattern formation. *Differentiation* 2003;71:1–17. [PubMed: 12558599]
20. Lemmen JG, Broekhof JLM, Kuiper GGJM, Gustafsson JA, Van Der Saag PT, van der Burg B. Expression of estrogen receptor α and β during mouse embryogenesis. *Mech Dev* 1999;81:163–167. [PubMed: 10330493]
21. Robinson GW, Karpf ABC, Kratochwil K. Regulation of mammary gland development by tissue interaction. *J Mammary Gland Biol Neoplasia* 1999;4:9–19. [PubMed: 10219903]
22. Hogg NA, Harrison CJ, Tickle C. Lumen formation in the developing mouse mammary gland. *J Embryol Exp Morphol* 1983;73:39–57. [PubMed: 6875464]
23. Soto, AM.; Lin, TM.; Justicia, H.; Silvia, RM.; Sonnenschein, C. An “in culture” bioassay to assess the estrogenicity of xenobiotics. In: Colborn, T.; Clement, C., editors. *Chemically induced alterations in sexual development: the wildlife/human connection*. Princeton: Princeton Scientific Publishing; 1992. p. 295-309.
24. Markey CM, Wadia PR, Rubin BS, Sonnenschein C, Soto AM. Long-term effects of fetal exposure to low doses of the xenoestrogen bisphenol-A in the female mouse genital tract. *Biol Reprod* 2005;72:1344–1351. [PubMed: 15689538]
25. Rubin BS, Lenkowski JR, Schaeberle CM, Vandenberg LN, Ronsheim PM, Soto AM. Evidence of altered brain sexual differentiation in mice exposed perinatally to low environmentally relevant levels of bisphenol A. *Endocrinology* 2006;147:3681–3691. [PubMed: 16675520]
26. Ziegler U, Groscurth P. Morphological features of cell death. *News Physiol Sci* 2004;19:124–128. [PubMed: 15143207]
27. Howard, CV.; Reed, MG. *Unbiased stereology*. Oxford, UK: BIOS Scientific Publishers; 1998.
28. vom Saal FS, Bronson FH. Sexual characteristics of adult female mice are correlated with their blood testosterone levels during prenatal development. *Science* 1980;208:597–599. [PubMed: 7367881]
29. vom Saal FS. Variation in phenotype due to random intrauterine positioning of male and female fetuses in rodents. *J Reprod Fertil* 1981;62:633–650. [PubMed: 7252935]
30. Ryan BC, Vandenberg JG. Intrauterine position effects. *Neurosci Biobehav Rev* 2002;26:665–678. [PubMed: 12479841]
31. Helledie T, Antonius M, Sorensen RV, Hertzog AV, Bernlohr DA, Kolvraa S, Kristiansen K, Mandrup S. Lipid-binding proteins modulate ligand-dependent trans-activation by peroxisome proliferator-activated receptors and localize to the nucleus as well as the cytoplasm. *J Lipid Res* 2000;41:1740–1751. [PubMed: 11060343]
32. Narbaitz R, Stumpf WE, Sar M. Estrogen receptors in the mammary gland primordia of fetal mouse. *Anat Embryol* 1980;158:161–166. [PubMed: 7356174]
33. Levine JF, Stockdale FE. Cell-cell interactions promote mammary epithelial cell differentiation. *J Cell Biol* 1985;100:1415–1422. [PubMed: 3886667]
34. Levine JF, Stockdale FE. 3T3-L1 adipocytes promote the growth of mammary epithelium. *Exp Cell Res* 1984;151:112–122. [PubMed: 6698114]
35. Beck JC, Hosick HL. Growth of mouse mammary epithelium in response to serum-free media conditioned by mammary adipose tissue. *Cell Biol Int Rep* 1988;12:85–97. [PubMed: 3396081]
36. Rudland PS, Twiston Davies AC, Tsao SW. Rat mammary preadipocytes in culture produce a trophic agent for mammary epithelia-prostaglandin E₂. *J Cell Physiol* 1984;120:364–376. [PubMed: 6589225]
37. Zangani D, Darcy KM, Shoemaker S, Ip MM. Adipocyte-epithelial interactions regulate the *in vitro* development of normal mammary epithelial cells. *Exp Cell Res* 1999;247:399–409. [PubMed: 10066368]

38. Sakakura T, Sakagami Y, Nishizuka Y. Dual origin of mesenchymal tissues participating in mouse mammary gland embryogenesis. *Dev Biol* 1982;91:202–207. [PubMed: 7095258]
39. Couldrey C, Moitra J, Vinson C, Anver M, Nagashima K, Green J. Adipose tissue: a vital *in vivo* role in mammary gland development but not differentiation. *Dev Dyn* 2002;223:459–468. [PubMed: 11921335]
40. Masuno H, Kidani T, Sekiva K, Sakayama K, Shiosaka T, Yamamoto H. Bisphenol A in combination with insulin can accelerate the conversion of 3T3–L1 fibroblasts to adipocytes. *J Lipid Res* 2002;43:676–684. [PubMed: 11971937]
41. Kimata K, Sakakura T, Inaguma Y, Kato M, Nishizuka Y. Participation of two different mesenchymes in the developing mouse mammary gland: synthesis of basement membrane components by fat pad precursor cells. *J Embryol Exp Morphol* 1985;89:243–257. [PubMed: 3912457]
42. Daniel CW, Berger JJ, Strickland P, Garcia R. Similar growth pattern of mouse mammary epithelium cultivated in collagen matrix *in vivo* and *in vitro*. *Dev Biol* 1984;104:57–64. [PubMed: 6734940]
43. Paszek MJ, Zahir N, Johnson KR, Lakins JN, Rozenberg GI, Gefen A, Reinhart-King CA, Margulies SS, Dembo M, Boettiger D, Hammer DA, Weaver VM. Tensional homeostasis and the malignant phenotype. *Cancer Cell* 2005;8:241–254. [PubMed: 16169468]
44. Neville MC, Medina D, Monks J, Hovey RC. The mammary fat pad. *J Mammary Gland Biol Neoplasia* 1998;3:109–116. [PubMed: 10819521]
45. Pennie WD, Aldridge TC, Brooks AN. Differential activation by xenoestrogens of ER α and ER β when linked to different response elements. *J Endocrinol* 1998;158:R11–R14. [PubMed: 9846177]
46. Kuiper GG, Lemmen JG, Carlsson B, Corton JC, Safe SH, Van Der Saag PT, van der Burg B, Gustafsson JA. Interaction of estrogenic chemicals and phytoestrogens with estrogen receptor β . *Endocrinology* 1998;139:4252–4263. [PubMed: 9751507]
47. Lemmen JG, Arends R, Van Der Saag PT, van der Burg B. *In vivo* imaging of activated estrogen receptors *in utero* by estrogens and bisphenol A. *Environ Health Perspect* 2004;112:1544–1549. [PubMed: 15531440]
48. Saji S, Jensen EV, Nilsson S, Rylander T, Warner M, Gustafsson JA. Estrogen receptors α and β in the rodent mammary gland. *Proc Natl Acad Sci USA* 2000;97:337–342. [PubMed: 10618419]
49. Wozniak AL, Bulayeva NN, Watson CS. Xenoestrogens at picomolar to nanomolar concentrations trigger membrane estrogen receptor- α -mediated Ca^{++} fluxes and prolactin release in GH3/B6 pituitary tumor cells. *Environ Health Perspect* 2005;113:431–439. [PubMed: 15811834]
50. Moriyama K, Tagami T, Akamizu T, Usui T, Saijo M, Kanamoto N, Hataya Y, Shimatsu A, Kuzuya H, Nakao K. Thyroid hormone action is disrupted by Bisphenol A as an antagonist. *J Clin Endocrinol Metab* 2002;87:5185–5190. [PubMed: 12414890]
51. Fang H, Tong W, Perkins R, Soto AM, Prechtel NV, Sheehan DM. Quantitative comparisons of *in vitro* assays for estrogenic activities. *Environ Health Perspect* 2000;108:723–729. [PubMed: 10964792]
52. Zoeller RT, Bansal R, Parris C. Bisphenol-A, an environmental contaminant that acts as a thyroid hormone receptor antagonist *in vitro*, increases serum thyroxine, and alters RC3/neurogranin expression in the developing rat brain. *Endocrinology* 2005;146:607–612. [PubMed: 15498886]
53. Sohoni P, Sumpter JP. Several environmental oestrogens are also anti-androgens. *J Endocrinol* 1998;158:327–339. [PubMed: 9846162]
54. Timms BG, Peterson SL, vom Saal FS. Prostate gland growth during development is stimulated in both male and female rat fetuses by intrauterine proximity to female fetuses. *J Urol* 1999;161:1694–1701. [PubMed: 10210442]
55. Clark MM, Bishop AM, vom Saal FS, Galef BG Jr. Responsiveness to testosterone of male gerbils from known intrauterine positions. *Physiol Behav* 1993;53:1183–1187. [PubMed: 8346303]
56. Nonneman DJ, Ganjam VK, Welshons WV, vom Saal FS. Intrauterine position effects on steroid metabolism and steroid receptors of reproductive organs in male mice. *Biol Reprod* 1992;47:723–729. [PubMed: 1477199]
57. vom Saal FS. The production of and sensitivity to cues that delay puberty and prolong subsequent oestrous cycles in female mice are influenced by prior intrauterine position. *J Reprod Fertil* 1989;86:457–471. [PubMed: 2760875]

58. McDermott NJ, Gandelman R, Reinisch JM. Contiguity to male fetuses influences ano-genital distance and time of vaginal opening in mice. *Physiol Behav* 1978;20:661–663. [PubMed: 567358]
59. vom Saal FS, Dhar MG. Blood flow in the uterine loop artery and loop vein is bidirectional in the mouse: implications for transport of steroids between fetuses. *Physiol Behav* 1992;52:163–171. [PubMed: 1529001]
60. Yeh S, Hu YC, Wang PH, Xie C, Xu Q, Tsai MY, Dong Z, Wang RS, Lee TH, Chang C. Abnormal mammary gland development and growth retardation in female mice and MCF7 breast cancer cells lacking androgen receptor. *J Exp Med* 2003;198:1899–1908. [PubMed: 14676301]
61. Drews U. Regression of mouse mammary gland Anlagen in recombinants of Tfm and wild-type tissues: testosterone acts via the mesenchyme. *Cell* 1977;10:401–404. [PubMed: 844099]
62. Gaido KW, Leonard LS, Lovell S, Gould JC, Babai D, Portier CJ. Evaluation of chemicals with endocrine modulating activity in a yeast-based steroid hormone receptor gene transcription assay. *Toxicol Appl Pharmacol* 1997;143:205–212. [PubMed: 9073609]
63. Rochefort H, Garcia M. Androgen on the estrogen receptor. I. Binding and *in vivo* nuclear translocation. *Steroids* 1976;28:549–560. [PubMed: 1006724]
64. Simpson ER. Aromatase: biologic relevance of tissue-specific expression. *Semin Reprod Med* 2004;22:11–23. [PubMed: 15083377]
65. vom Saal FS, Grant WM, McMullen CW, Laves KS. High fetal estrogen concentrations: correlation with increased adult sexual activity and decreased aggression in male mice. *Science* 1983;220:1306–1309. [PubMed: 6857252]
66. Greco TL, Payne AH. Ontogeny of expression of the genes for steroidogenic enzymes P450 side-chain cleavage, 3 β -hydroxysteroid dehydrogenase, P450 17 α -hydroxylase/C17-20 lyase, and P450 aromatase in fetal mouse gonads. *Endocrinology* 1994;135:262–268. [PubMed: 8013361]
67. Mannan MA, O'Shaughnessy PJ. Steroidogenesis during postnatal development in the mouse ovary. *J Endocrinol* 1991;130:101–106. [PubMed: 1880470]
68. Nunez EA, Benassayag C, Savu L, Vallette G, Delorme J. Oestrogen binding function of α 1-fetoprotein. *J Steroid Biochem* 1979;11:237–243. [PubMed: 90750]
69. Markey CM, Michaelson CL, Veson EC, Sonnenschein C, Soto AM. The mouse uterotrophic assay: a re-evaluation of its validity in assessing the estrogenicity of bisphenol A. *Environ Health Perspect* 2001;109:55–60. [PubMed: 11171525]
70. Bern, HA. The fragile fetus. In: Colborn, T.; Clement, C., editors. *Chemically induced alterations in sexual and functional development: the wildlife/human connection*. Princeton: Princeton Scientific Publishing Co. Inc.; 1992. p. 9-15.

Abbreviations

ALBP	Adipocyte lipid binding protein
BPA	bisphenol-A
BW	body weight
E	embryonic day
ER	estrogen receptor
PPAR	peroxisomal proliferator-activated receptor

**Fig. 1.**

Effects of intrauterine position on the growth of the mammary ductal tree in control and BPA-exposed fetuses. A, Whole mount of control 0M female mammary gland. B, Whole mount of BPA-exposed 0M female mammary gland. Note the increased size of the epithelial cords, compared with controls. C, Number of branching points was increased in control 1M (gray) and 2M (violet) females, compared with 0M (green) females. In BPA-exposed females, 0M females were as developed as 1M and 2M females. D, Area subtended by the ductal tree was increased in control 2M females, compared with 0M females. These position-specific effects disappeared after BPA exposure. E, Ductal extension was significantly increased in 1M females exposed to BPA, compared with 1M control females. Scale bar, 100 μ m. n = 8–15/positional group for both treatments. *, $P < 0.045$, **, $P < 0.03$, ***, $P < 0.025$.

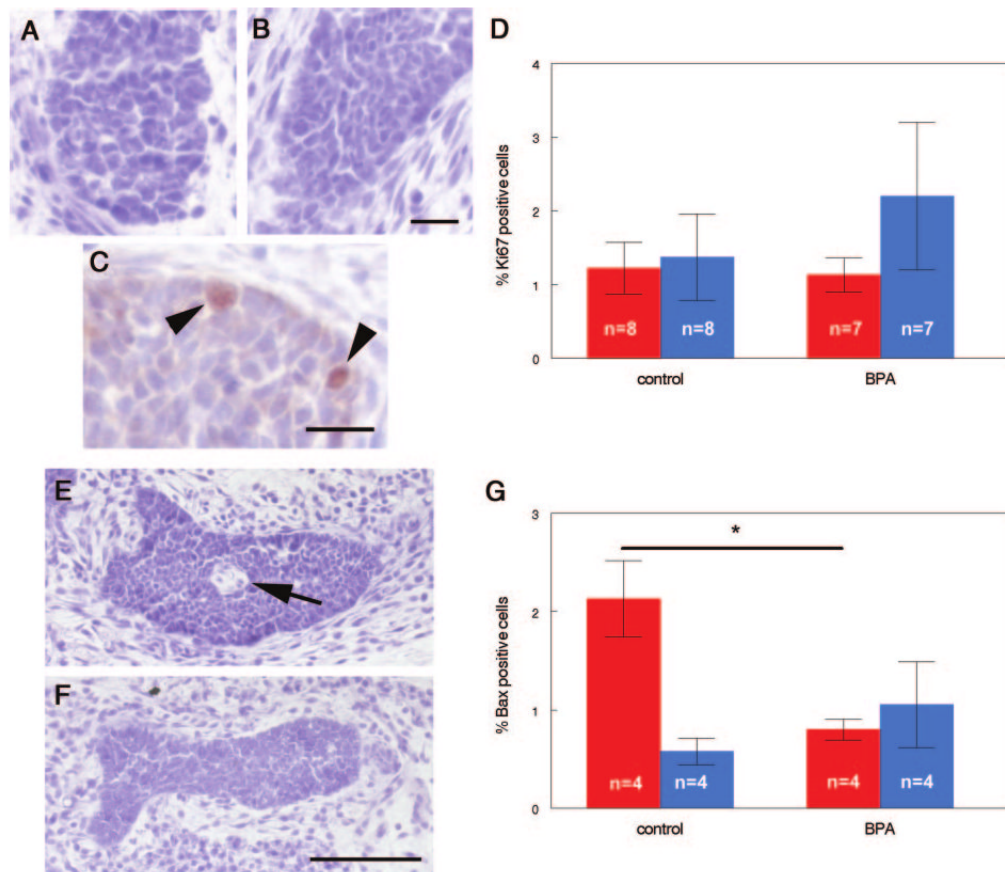
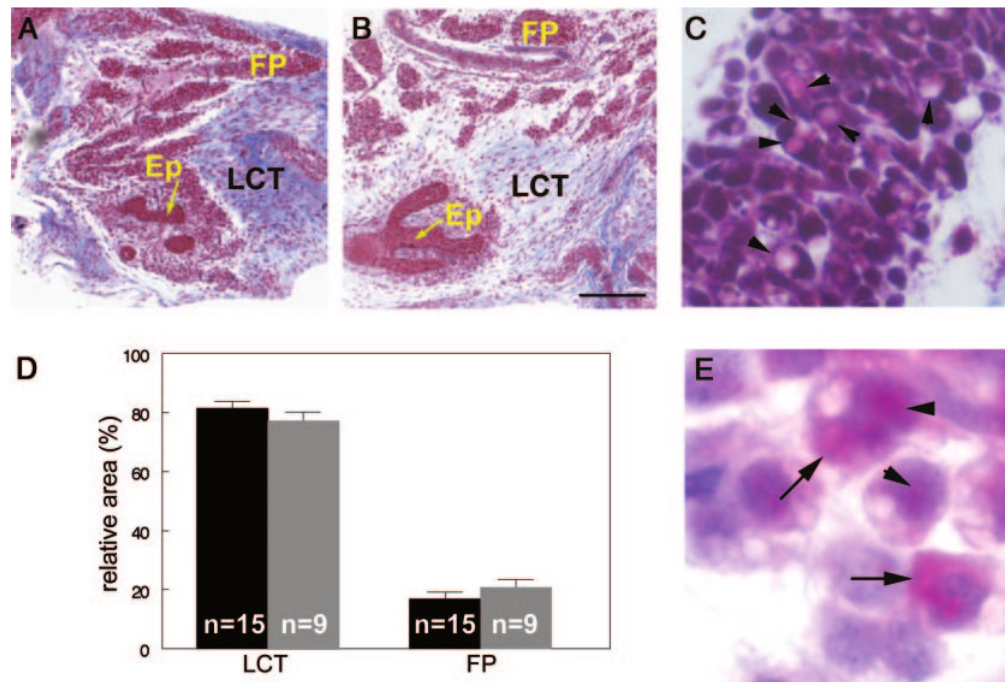
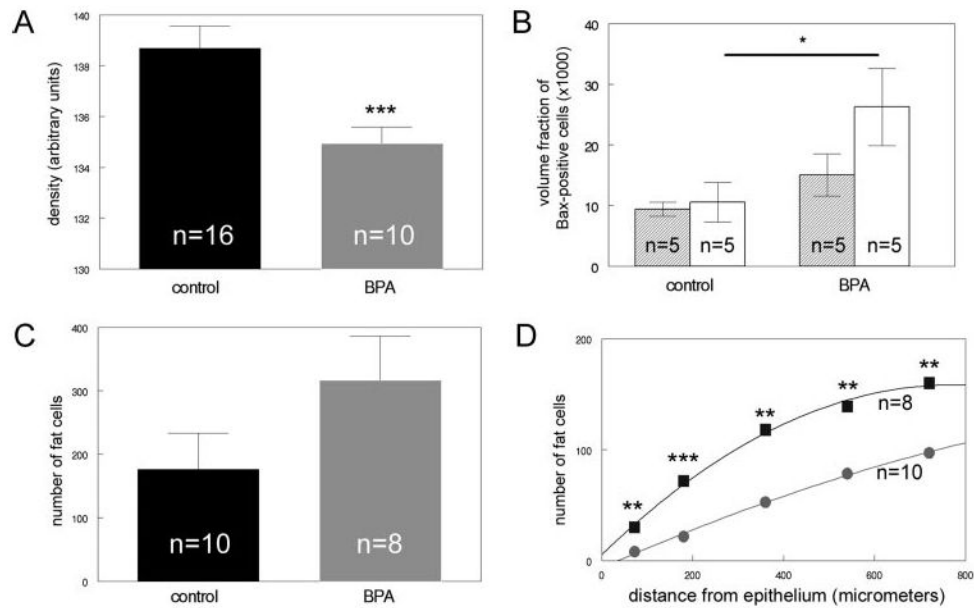


Fig. 2. Development of the mammary epithelium in control and BPA-exposed females. Epithelial cells are larger and more heterogeneous in shape and size in control animals (A), compared with BPA-exposed (B). C, Ki67 expression in epithelium from a control fetus (*arrowheads* indicate positive cells). D, Distribution of Ki67-positive cells in the inner (*red*) and outer cord cells (*blue*) was similar for both treatments. E, Lumen formation (*arrow*) was observed in 38% of control animals but in none of the BPA-exposed animals (F). G, Expression of proapoptotic marker Bax was significantly decreased in the inner cord cells (*red*) of BPA-exposed relative to controls, but there were no differences in Bax expression in the outer cord cells (*blue*) by treatment. Scale bars (B and C), 20 μm ; (F), 100 μm . *, $P = 0.021$.

**Fig. 3.**

Appearance of the mammary stroma in control and BPA-exposed females. Masson's Trichrome staining of control (A) and BPA-exposed (B) E18 mammary glands. C, Clear vacuoles (arrowheads) are observed in some cells within the developing fat pad. D, The relative area of loose connective tissue and fat pad are similar in control (black) and BPA-exposed (gray) mammary glands. E, Localization of ALBP in cells of the fat pad in the nuclear (arrowheads) and cytoplasmic (arrows) compartments of adipocytes. Ep, Epithelium, FP, fat pad, LCT, loose connective tissue. Scale bar, 200 μ m.

**Fig. 4.**

Alterations are observed in the developing fat pad of BPA-exposed females, compared with controls. A, The OD of the fat pad in BPA-exposed animals (*gray*) is decreased, compared with controls (*black*). B, Expression of the proapoptotic marker Bax is significantly increased in the developing fat pad (*white*) in BPA-exposed animals relative to controls. No statistically significant differences were noted in the loose connective tissue (*shaded*). C, The total number of cells containing fat vacuoles was increased in BPA-exposed females, compared with controls, although this increase was not significant. D, The number of adipocytes was significantly increased within 1 mm from the developing epithelium in BPA-exposed females (*squares*), compared with controls (*circles*). *, $P < 0.05$; **, $P < 0.02$; ***, $P < 0.005$.

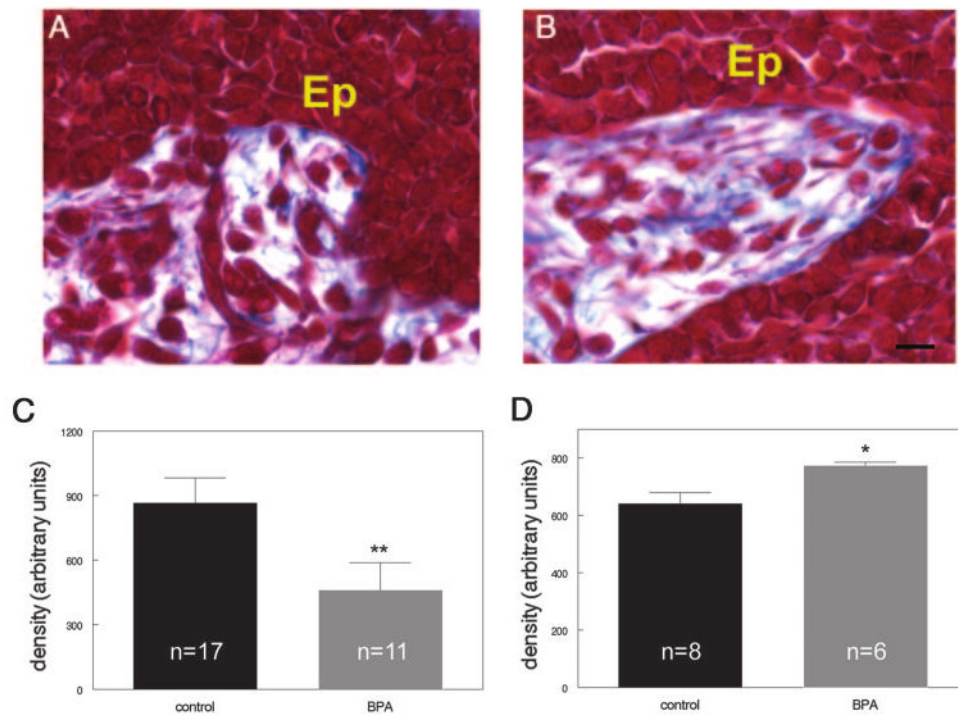


Fig. 5. BPA exposure alters collagen localization in the fetal mammary gland. Masson's Trichrome staining of control (A) and BPA-exposed (B) E18 mammary glands. Note the increase in blue collagen fibers directly abutting the epithelium in BPA-exposed mammary glands. C, The density of collagen in the entire stromal compartment is significantly decreased in BPA-exposed females, compared with controls. D, The density of collagen within 10 μm of the epithelial ducts is significantly increased in BPA-exposed females. [Ep, Epithelium; *blue*, collagen fibers. *Scale bar*, 10 μm]. *, $P = 0.042$; **, $P = 0.010$.

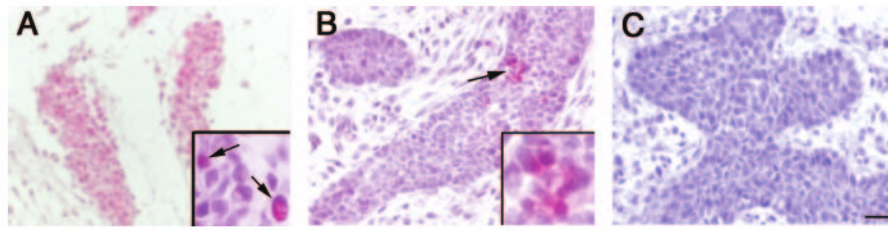


Fig. 6. ER α is expressed in the E18 mammary gland. A, ER α expression in the developing fat pad. *Inset* shows higher magnification (*arrows* indicate positive cells). B, Punctate expression of ER α (*arrows* indicate positive cells) is observed in some epithelial cords at E18. *Inset* shows higher magnification of positive cells. C, Negative control, E18 mammary gland treated in the same way as A and B but without the addition of primary antibody. *Scale bar*, 100 μ m.

Table 1

Growth parameters of the E18 mammary gland

Parameter	Control (mean \pm SEM) n = 40	BPA (mean \pm SEM) n = 36
Ductal area	0.098 \pm 0.004 mm ²	0.116 \pm 0.008 mm ^{2a}
Area subtended by ductal tree	0.197 \pm 0.012 mm ²	0.244 \pm 0.024 mm ²
Ductal extension	0.741 \pm 0.018 mm	0.835 \pm 0.030 mm ^a
Number of tertiary branches	3.03 \pm 0.34	3.94 \pm 0.49
Length of the primary duct	0.373 \pm 0.017 mm	0.430 \pm 0.033 mm
Branching points	3.0 \pm 0.21	3.61 \pm 0.366
Number of terminal ends	4.0 \pm 0.23	4.5 \pm 0.339

^aSignificant differences between control and BPA-exposed animals.

Table 2

Expression of mRNA in the E18 mammary gland by quantitative RT-PCR

	Control E18 mammary gland (n = 4–6)	BPA E18 mammary gland (n = 4–6)
ER α	0.0359 \pm 0.0109	0.0321 \pm 0.0132
ER β	0.1126 \pm 0.0975	0.0542 \pm 0.0250
ALBP	0.218 \pm 0.026	0.273 \pm 0.028
Collagen I	3.252 \pm 0.416	3.174 \pm 0.401
PPAR γ	2.148 \pm 0.257	2.184 \pm 0.322